Experimental Study on Frequency Support of Variable Speed Wind Turbine Based on Electromagnetic Coupler

Rui You[*], Jianyun Chai[**], Xudong Sun[**], Daqiang Bi[**], and Xinzhen Wu[†]

[*],[†]Department of Electrical Engineering, Qingdao University, Qingdao, China
[**]Department of Electrical Engineering, Tsinghua University, Beijing, China

Abstract

In the variable speed Wind Turbine based on ElectroMagnetic Coupler (WT-EMC), a synchronous generator is coupled directly to the grid. Therefore, like conventional power plants, WT-EMC is able to inherently support grid frequency. However, due to the reduced inertia of the synchronous generator, WT-EMC is expected to be controlled to increase its output power in response to a grid frequency drop to support grid frequency. Similar to the grid frequency support control of Type 3 or Type 4 wind turbine, inertial control and droop control can be used to calculate the WT-EMC additional output power reference according to the synchronous generator speed. In this paper, an experimental platform is built to study the grid frequency support from WT-EMC with inertial control and droop control. Two synchronous generators, driven by two induction motors controlled by two converters, are used to emulate the synchronous generators in conventional power plants and in WT-EMCs respectively. The effectiveness of the grid frequency support from WT-EMC with inertial control and droop control responding to a grid frequency drop is validated by experimental results. The selection of the grid frequency support controller and its gain for WT-EMC is analyzed briefly.

Key words: Droop control, Experimental platform, Frequency support, Inertial control, Synchronous generator, Variable speed wind turbine

I. INTRODUCTION

Nowadays grid frequency is stabilized by the synchronous generators in conventional power plants [1]. When a power imbalance occurs in the grid, such as a sudden load change, the synchronous generator electromagnetic torque changes instantaneously. This leads to a mismatch between the mechanical torque and electromagnetic torque of the synchronous generator, and the synchronous generator speed and kinetic energy stored in the rotor change. The change of kinetic energy limits the rate of change of frequency (ROCOF). The ROCOF value is determined by the system inertia, which is the sum of all synchronous generator inertia. The lower the system inertia, the higher the ROCOF value after a power

imbalance [2]. In a conventional power plant, the speed error signal between the measured generator speed and its reference speed is amplified and integrated to generate a control signal, which actuates the main steam supply valves in a steam turbine, or the gates in a hydraulic turbine. As a result, the synchronous generator mechanical torque changes at a slow rate due to the large rotor inertia, which leads to decayed changes of the synchronous generator speed and grid frequency [3].

The worldwide concern about the environment has led to the rapid development of wind energy. Wind turbine technology has developed from constant-speed constant-frequency to Variable-Speed Constant-Frequency (VSCF). The rotor speed is regulated with the wind speed change for VSCF wind turbines to achieve the maximum wind power capture [4], [5]. Type 3 (with a doubly fed asynchronous generator) and Type 4 (with a full scale power converter) wind turbines are widely used as VSCF wind turbines [6]. For these turbines, the use of power electronic converter (partially) decouples the generator speed and grid frequency, resulting in reductions of the power system inertia [7], [8]. Reduced system inertia is a particular

concern to transmission system operators, especially in areas where a large number of synchronous generators are displaced by VSCF wind turbines. Therefore, for VSCF wind turbines, supplementary power is expected to be generated in response to grid frequency drops to support the grid frequency [9]. During grid frequency support for Type 3 and Type 4 wind turbines, the additional power reference is calculated based on the measured grid frequency, mainly in two ways: inertial control and droop control [10]-[12]. The additional power is calculated according to the grid frequency derivative df/dt in the first method, and according to the grid frequency deviation from the nominal value in the second method [13], [14].

A novel VSCF wind turbine—variable speed Wind Turbine based on ElectroMagnetic Coupler (WT-EMC) was proposed in [15]. A synchronous generator is coupled to the grid directly and an ElectroMagnetic Coupling speed regulating Device (EMCD) is used to connect the gearbox high speed shaft and the synchronous generator rotor shaft, to transmit captured wind power to the synchronous generator. Compared with Type 3 and Type 4 wind turbines, the synchronous generator is directly coupled to the grid in WT-EMC, which makes this wind turbine have better capabilities in terms of transient overload, fault ride-through and grid voltage support in the aspect of grid voltage control, as verified in [16]. It also has better inherent grid frequency support capability in terms of grid frequency support, as verified in [17]. However, the electromagnetic coupler decouples the synchronous generator side and gearbox side of the drive train, which results in a limited inherent grid frequency support capability that needs to be enhanced. Therefore, WT-EMC is expected to be controlled to generate additional power in response to a grid frequency drop to support the grid frequency. For WT-EMC, the synchronous generator speed is more stable than the grid frequency which is used in the grid frequency support controller for Type 3 and Type 4 wind turbines. Thus, it is used as the input signal to calculate the additional power reference during grid frequency support. The existence of the WT-EMC inherent grid frequency support capability and the effectiveness of the two designed controllers (inertial controller and droop controller) are confirmed with the simulation results in [17].

In this paper, an experimental platform is built to study the grid frequency support from WT-EMC. Two synchronous generators driven by two induction motors are used to emulate the synchronous generators in conventional power plants and WT-EMCs respectively. The two induction motors are controlled by two converters, whose torque commands are calculated for the corresponding control. The main contributions in this paper are presented below. The effectiveness of the grid frequency support from WT-EMC with two controllers responding to a grid frequency drop, implemented by connecting a new load is validated with experimental results. The improvement in the grid frequency from WT-EMC with

the inertial controller and droop controller is compared. The selection of the grid frequency support controller and its gain for WT-EMC is analyzed based on experimental results. A wind farm consisting of WT-EMCs with a supplementary grid frequency support controller is expected to contribute to grid inertia similarly to the synchronous generator in a conventional power plant with a similar rating.

The rest of the paper is organized as follows. Section II briefly introduces WT-EMC and its grid frequency support controllers: inertial controller and droop controller. Section III describes the experimental platform built in terms of its hardware and software in detail. Section IV presents the experiments and experimental results. Section V concludes the analysis.

II. WT-EMC AND ITS FREQUENCY SUPPORT CONTROLLER

In WT-EMC, an EMCD is used to connect the gearbox high speed shaft and the synchronous generator rotor shaft, and to transmit the captured wind power to the synchronous generator. The structure of the EMCD currently used is shown in Fig. 1. It is composed of an electromagnetic coupler and a converter. The electromagnetic coupler is essentially a squirrel cage induction motor. Unlike a common one with only one revolving shaft, the two shafts of the electromagnetic coupler rotate. The converter is used to control the relative speed between the two shafts and the electromagnetic torque of the electromagnetic coupler. The back shaft speed is always higher than the front shaft speed in WT-EMC. Only a one quadrant operation converter with only 1/6 of the wind turbine rated capacity is needed [18]. The mechanical torque of the synchronous generator in WT-EMC is applied by the converter. Therefore, a quick change of the mechanical torque on the synchronous generator rotor can be achieved and it is highly controllable, which is different from the synchronous generators used in conventional power plants [19]. A 1.5 MW experimental platform whose drive train is composed of an induction motor used to emulate blades and a gearbox, an electromagnetic coupler and a synchronous generator was built. From the experimental results it can be observed that WT-EMC can operate normally under various operating conditions. The EMCD transmission efficiency is high. It can reach up to 98% at the rated condition [20]. For the electromagnetic coupler built, the length is 2.5 m and the weight is 6.5 tons. According to preliminary calculations, the cost of a 1.5 MW WT-EMC is similar to that of a Type 3 wind turbine with the same power rating.

The WT-EMC structure and its control are illustrated in detail in Fig. 2. During normal operation, the converter torque command T^* is calculated with the front shaft speed ω_f and the predefined wind turbine optimal torque-speed curve to
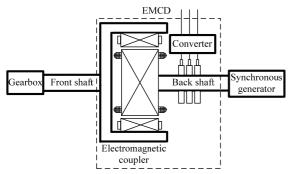
Fig. 1. Schematic diagram of the EMCD structure.

achieve the maximum wind power capture. In the de-load mode, T^* is calculated according to the WT-EMC output power command from wind farm [21]. When a power imbalance occurs and leads to changes of the synchronous generator speed and grid frequency, the converter torque command calculation is switched to the grid frequency support mode. During grid frequency support, the torque command is calculated with controllers designed to regulate the output power of WT-EMC so as to improve the grid frequency dynamic characteristic. Once the grid frequency support finishes, the torque command calculation is switched back to the normal mode and WT-EMC returns to the original operation mode. A pitch controller is used to reduce the power imbalance between the captured wind power and the output electrical power of WT-EMC.

For Type 3 and Type 4 wind turbines, the grid frequency is the input signal of the frequency support controller. This raises some challenges, because the calculation of the grid frequency is sensitive to grid harmonics and disturbances. In the case of WT-EMC, the synchronous generator speed is synchronous to the grid frequency, offering a far more stable and accurately measured reference as the input signal of the grid frequency support controller. This is an important advantage that WT-EMC has compared with Type 3 and Type 4 wind turbines. Therefore, the back shaft speed ω_b (synchronous generator speed in WT-EMC) is used as the input signal of the grid frequency support controller for WT-EMC. An inertial controller or droop controller is used for grid frequency support based on the back shaft speed.

A. Inertial Controller

In a conventional power plant, the kinetic energy of the synchronous generator rotor is immediately released once the grid frequency drops. The kinetic energy E stored in the rotor is expressed as:

$$E = \frac{1}{2}J\omega_m{}^2 \qquad (1)$$

where ω_m is the generator speed and J is the moment of inertia. The power P, extracted from the rotating rotor, is [1]:

$$P = \frac{dE}{dt} = J\omega_m\frac{d\omega_m}{dt} \qquad (2)$$

The inertia constant H is defined as:

$$H = \frac{J\omega_s^2}{2S} \qquad (3)$$

where ω_s is the synchronous speed and S is the generator rated apparent power. The per-unit value of the power $\overline{P}$ can be calculated as [22]:

$$\overline{P} = \frac{P}{S} = 2H\frac{\omega_m}{\omega_s}\frac{d(\omega_m / \omega_s)}{dt} = 2H\overline{\omega_m}\frac{d\overline{\omega_m}}{dt} \qquad (4)$$

where $\overline{\omega_m}$ is the per-unit value of the generator speed. During grid frequency support, the WT-EMC additional power reference $\overline{\Delta P_{in}}$ is calculated with an inertial controller according to the per-unit value of the back shaft speed $\overline{\omega_b}$. This can be expressed as:

$$\overline{\Delta P_{in}} = K_{in}\overline{\omega_b}\frac{d\overline{\omega_b}}{dt} \qquad (5)$$

where K_{in} is the inertial controller gain which is analogous to $2H$.

B. Droop Controller

In a conventional power plant, a governor with the droop characteristic is widely used to share the load change for synchronous generators in proportion to their ratings [3]. The droop characteristic is illustrated as [11]:

$$\overline{\Delta P} = \frac{\overline{\Delta\omega}}{R} \qquad (6)$$

where $\overline{\Delta P}$ and $\overline{\Delta\omega}$ are the per-unit values of the synchronous generator power change and its speed change respectively. R is the droop. During grid frequency support, the WT-EMC additional power reference $\overline{\Delta P_{dr}}$ is calculated with a droop controller according to $\overline{\omega_b}$, which is expressed as [17]:

$$\overline{\Delta P_{dr}} = K_{dr}(\overline{\omega_b} - 1) \qquad (7)$$

where K_{dr} is the droop controller gain.

III. INTRODUCTION OF THE EXPERIMENTAL PLATFORM

An isolated grid experimental platform is built to validate the effectiveness of the grid frequency support from WT-EMC with an inertial controller or droop controller above. The structure of the experimental platform is shown in Fig. 3. The isolated grid is composed of resistive loads and two power sources: Synchronous Generator1 (SG1) and Synchronous Generator2 (SG2). Load1 (L1) is selected as 3 kW (three phases, 1 kW per phase when the line-line supply voltage is 380 V). Load2 (L2) is 660 W (three phases, 220 W per phase when the line-line supply voltage is 380 V). The rated capacities of SG1 and SG2 are 30 kW and 7.5 kW respectively. SG1 and SG2 are both brushless excitation 4
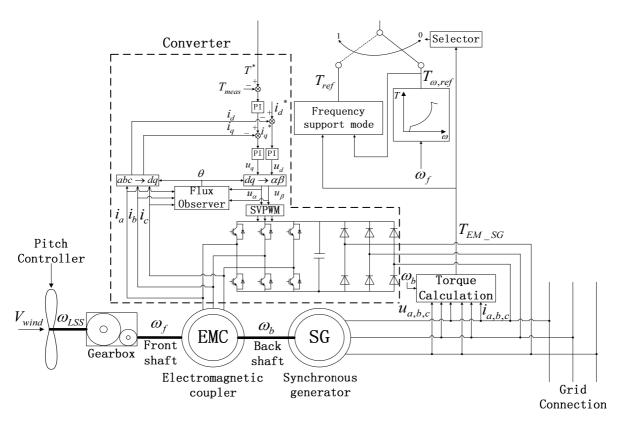
Fig. 2. WT-EMC structure and control.

pole synchronous generators. Their rated voltages are both 380 V and their rated speeds are both 1500 rpm. Two automatic voltage regulators are equipped for SG1 and SG2 to stabilize their terminal voltages. SG1 is driven by Induction Motor1 (IM1) which is controlled by Converter1. SG2 is driven by Induction Motor2 (IM2) which is controlled by Converter2. Converter1 and Converter2 are both supplied from the grid. SG1 is used to emulate the synchronous generators in conventional power plants, whose speed governor characteristics are emulated with changes of Converter1 torque command according to SG1 speed. Because a synchronous generator is directly coupled with the grid and its mechanical torque is applied by a converter for WT-EMC, which is also true for SG2 (directly coupled with the isolated grid, whose mechanical torque is applied by Converter2), SG2 is used to emulate the synchronous generators in WT-EMCs. Power Measurement module1 (PM1) and Power Measurement module2 (PM2) are used to measure the active powers where they are placed (measurements for the total power consumed by the loads and SG2 output power respectively). A synchronizing device is used to finish SG2 connection to the isolated grid.

The software of the experimental platform built is mainly composed of a Human Machine Interface (HMI), a communication program between a computer and different devices, like converters and power measurement modules, and a data storage program. LabVIEW is used to develop the
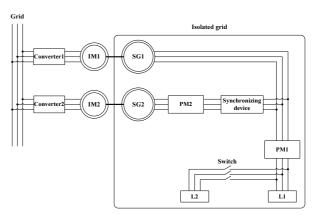

Fig. 3. Structure of the experimental platform built.

HMI, where the operating conditions of devices can be displayed and experiments can be programmed and controlled [23]. The communication between different devices and a computer is achieved with RS-485 and the Modbus RTU protocol. A photo of the experimental platform built is shown in Fig. 4. The solid lines indicate the actual three phase wires. Dotted arrows are used to show the names of the devices.

IV. EXPERIMENTAL RESULTS

SG1 droop control (SG1 input power and its speed meet the designed droop relationship) is implemented via the torque
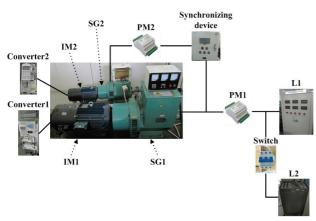
Fig. 4. Photo of the experimental platform built.

Fig. 5. SG1 speed.

command regulation of Converter1. The first experiment is designed to validate the effectiveness of the SG1 droop control and to analyze the isolated grid frequency drop after a load change.

Then, experiments are done to validate the effectiveness of the grid frequency support from WT-EMC with an inertial controller or droop controller. Firstly, the control modes of Converter1 and Converter2 are both set speed control modes. With a gradual change of the speed command from 0 to 1500 rpm for Converter1 and Converter2, SG1 and SG2 are controlled to gradually accelerate to 1500 rpm. Then, Load1 is connected to be fed by SG1. The Converter2 speed command is adjusted dynamically according to the speed regulation indicator of the synchronizing device. Once the voltage difference and phase difference measured between SG1 and SG2 are within allowable ranges, the grid connection switch, inside the synchronizing device in Fig. 4, is automatically closed and the control mode of Converter2 is immediately switched from the speed control mode to the torque control mode. Then, the Converter2 torque command is increased gradually to increase the SG2 output power to 1/5 of the power consumed by Load1 so the output power ratio between SG1 and SG2 is 4:1. This is the same ratio as their rated capacities ratio. Then, the Converter1 control mode is switched to the torque control mode and its initial torque command is set to the steady torque value before its control mode switch. The isolated grid frequency is 50 Hz and the line-line voltage is then 380 V. A droop whose value is 1.11, which is much higher than the one used in conventional power plants, is implemented to calculate the Converter1 torque command. This is because the employed high droop value can avoid the SG1 speed divergent oscillation and improve system stability. At last, Load2 is connected to the isolated grid with the switch at 10 s. The SG2 mechanical torque is calculated with an inertial controller or droop controller, and applied via the torque command regulation of Converter2.

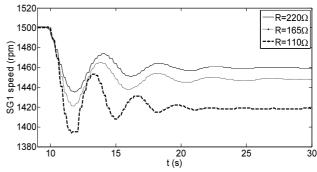If WT-EMC operates in the de-load mode with enough power reserve, the additional power generated is from the increased wind power captured with a decrease in the pitch angle, and the rotor speed can be kept almost constant during grid frequency support. Therefore, after the grid frequency support, WT-EMC output power is controlled to gradually reduce to its original value, and there is no period when its output power is lower than its original value to make the rotor accelerate. In order to focus on the grid frequency dynamic characteristic improvement with an inertial controller or droop controller, SG2 is controlled to increase its output power during grid frequency support with the controller and then to gradually reduce its output power to its original value. This emulates that WT-EMC operates in the de-load mode with enough power reserve. Experimental results are presented below.

A. One Synchronous Generator Response to a Load Change

In the first experiment, SG2 is not connected to the isolated grid and Load1 is only fed by SG1. Then, Load2 is connected at 10 s. The SG1 speed characteristic for different Load2 resistance values R is shown in Fig. 5. It can be seen that the larger the Load2 (the smaller resistance value R) that is connected, the worse characteristic of the isolated grid frequency that is proportional to the SG1 speed becomes in terms of the frequency nadir and ROCOF.

The corresponding SG1 output power and Converter1 torque (command value and actual value) are shown in Fig. 6 and 7 respectively. In Fig. 7, the Converter1 torque command and the actual torque applied are displayed by the black curves and gray curves respectively. In this experiment, the isolated grid voltage is almost constant due to the SG1 automatic voltage regulator, except for the period when the frequency nadir occurs with $R=110\,\Omega$ in Fig. 5, due to the too low SG1 speed. When the voltage is almost constant, the connection of Load2 leads to a sudden increase of the SG1 output power and the SG1 output power increase is equal to the power consumed by Load2. The larger the Load2 that is connected, the higher SG1 output power increases, as shown in Fig. 6. This results in a higher power imbalance between the SG1 input mechanical power and its output electrical power. The SG1 power imbalance leads to a decline in the SG1 speed (isolated grid frequency), and the Converter1
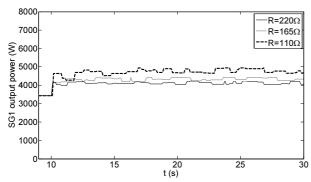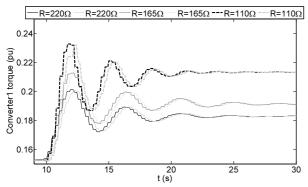
Fig. 6. SG1 output power.

Fig. 7. Converter1 torque command and actual torque applied.

torque command is increased with the droop designed, as shown in Fig. 7. The LabVIEW program execution time, the communication time between the computer and Converter1, and the Converter1 torque response time result in a time delay between the Converter1 torque command and the actual mechanical torque applied on SG1. As a result, the governor characteristic in conventional power plants is successfully emulated.

B. Inertial Controller

The SG2 speed ω is used as the inertial controller input signal. The additional power reference ΔP is calculated below:

$$\Delta P = \frac{K}{1960} \omega \frac{d\omega}{dt} \qquad (8)$$

The SG1 speed, which is proportional to the isolated grid frequency, is shown in Fig. 8 when an inertial controller with different gains K is used. The gray solid curve is the speed when the SG2 input power is kept constant. This emulates the WT-EMC normal operation without an additional grid frequency support controller. The speed curves are illustrated by the gray dashed, black dotted and black solid curves with different gain values K when an inertial controller is used. The corresponding mechanical torque on SG2, which is applied by Converter2, the SG2 output power and the SG1 output power are shown in Fig. 9, 10 and 11 respectively. During grid frequency support, the SG2 additional power reference is calculated according to equation (8) with an
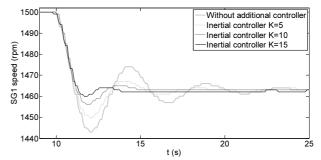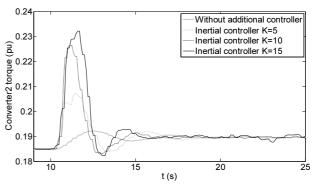

Fig. 8. SG1 speed.
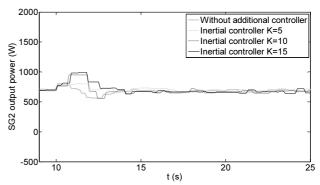

Fig. 9. Torque on SG2 applied by Converter2.
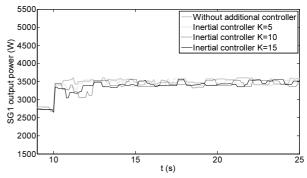

Fig. 10. SG2 output power.

Fig. 11. SG1 output power.

inertial controller. SG2 is controlled to increase its output power via an increase of the mechanical torque on SG2 applied by Converter2, which can be seen in Fig. 9 and 10. The increase of the SG2 output power reduces the SG1 output power change and the SG1 power imbalance between its
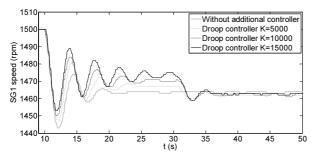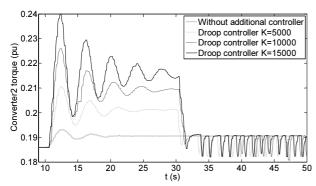
Fig. 12. SG1 speed.

Fig. 13. Torque on SG2 applied by Converter2.

Fig. 14. SG2 output power.

Fig. 15. SG1 output power.

input mechanical power and output electrical power, as shown in Fig. 11. Therefore, the dynamic characteristic of the SG1 speed (isolated grid frequency) is improved. From Fig. 8, 9, 10 and 11, it can be seen that the higher K is used, the higher the SG2 output power and the lower the SG1 output power and power imbalance can be achieved. This results in a better improvement of the frequency dynamic characteristic, especially the frequency nadir.

C. Droop Controller

The additional power reference ΔP is calculated below with a droop controller.

$$\Delta P = \frac{K}{1960}(1500 - \omega) \qquad (9)$$

The SG1 speed for different gains K in the droop controller is shown in Fig. 12. The corresponding mechanical torque on SG2, which is applied by Converter2, the SG2 output power and the SG1 output power are shown in Fig. 13, 14 and 15 respectively. The grid frequency support period is set to 20 s. During grid frequency support, the SG2 additional power reference is calculated according to equation (9) with a droop controller. The higher the gain K that is used, the higher the SG2 output power, the lower the SG1 output power and the better the improvement of the isolated grid frequency (proportional to SG1 speed in Fig. 12) dynamic characteristic. In particular, the frequency nadir can be achieved. After the grid frequency support (after 30 s), SG2 is controlled to reduce its output power to its original value gradually via a gradual decrease of the mechanical torque on SG2, which is applied by Converter2, as shown in Fig. 13. Then, in order to
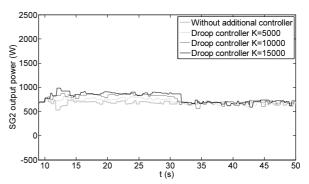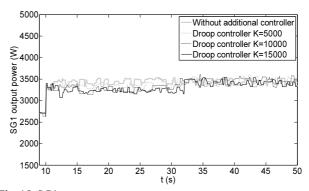
keep the SG2 output power almost constant, the mechanical torque on SG2 applied by Converter2 is controlled to change according to the SG2 speed, as shown by the torque oscillation after 33 s in Fig. 13. However, the stable operation of the isolated grid is not affected.

The isolated grid inertia is very small, since only the rotors of IM1, SG1, IM2 and SG2 contribute to it. Therefore, its frequency drops very fast after the connection of Load2 in the experiments above. It can be seen that from 10 s to about 12 s the isolated grid frequency, proportional to the SG1 speed shown by the gray solid curves in Fig. 8 and 12, drops because of the power imbalance. Although the time for the SG2 output power change (about 2 s) is very short, the experimental results show that SG2 has been controlled to generate additional power fast enough to successfully support the grid frequency with the two controllers, resulting in an obvious improvement of the frequency nadir and a marginal improvement of the ROCOF. Therefore, in a real grid whose inertia is much higher than the one of the isolated grid built, more time is left for the WT-EMC output power change and an inertial controller or droop controller can be used for WT-EMC to generate additional power in response to a grid frequency drop.

Overall, it can be seen from the above experimental results that the effectiveness of grid frequency support from WT-EMC with an inertial controller and droop controller has been validated. Responding to a grid frequency drop, an increase of the WT-EMC output power with the two controllers reduces the synchronous generator output power

change and the power imbalance between the input mechanical power and the output electrical power in conventional power plants. Therefore, the dynamic characteristics of the synchronous generator speed and grid frequency are improved. From a comparison of the obtained experimental results with the two controllers based on the built isolated grid, it can be seen that the frequency oscillates less and reaches its steady value faster with the inertial controller after a new load connection. The output power change with the inertial controller is less than that with the droop controller for a similar improvement of the frequency nadir. One or both of the two controllers can be used to support the grid frequency. The selection of the two controllers and their gains should be done in accordance with the grid characteristic, wind speed, impact on the wind turbine structural loads, etc.

V.   CONCLUSIONS

WT-EMC has inherent grid frequency support capability due to the fact that its synchronous generator is directly coupled to the grid. Nevertheless, the WT-EMC drive train structure leads to its small inertia when compared with conventional power plants. Therefore, WT-EMC is expected to be controlled to increase its output power to improve the frequency dynamic characteristic when the grid frequency drops. Inertial and droop controllers are used to calculate the additional power reference during the grid frequency support according to the synchronous generator speed in WT-EMC. An experimental platform has been built to validate the effectiveness of the WT-EMC inertial controller and droop controller for grid frequency support. Experimental results have shown that an increase of the WT-EMC output power with an inertial controller or droop controller reduces the synchronous generator output power change and the power imbalance between its input mechanical power and output electrical power in conventional power plants. This results in the dynamic characteristic improvements of the synchronous generator speed and grid frequency. Therefore, the introduction of WT-EMC does not reduce the grid inertia, as long as additional controllers such as an inertial controller or droop controller are implemented on it.

REFERENCES

[1] J. Morren, J. Pierik, and S. W. H. de Haan, "Inertial response of variable speed wind turbines," *Electric Power Systems Research*, Vol. 76, No. 11, pp. 980-987, Jul. 2006.

[2] J. Villena-Lapaz, A. Vigueras-Rodriguez, E. Gomez-Lazaro, A. Molina-Garcia, and J. A. Fuentes-Moreno, "Evaluation of frequency response of variable speed wind farms for reducing stability problems in weak grids," in *IEEE Power Electronics and Machines in Wind Applications (PEMWA)*, pp. 1-5, Jul. 2012.

[3] P. Kundur, *Power System Stability and Control*, McGraw-Hill, pp. 581-626, 1994.

[4] Y. Liu, Q. H. Wu, and X. X. Zhou, "Co-ordinated multiloop switching control of DFIG for resilience enhancement of wind power penetrated power systems," *IEEE Trans. Sustain. Energy*, Vol. 7, No. 3, pp. 1089-1099, Jul. 2016.

[5] H. Li and Z. Chen, "Overview of different wind generator systems and their comparisons," *IET Renewable Power Generation*, Vol. 2, No. 2, pp. 123-138, Jun. 2008.

[6] Wind turbines — Part 27-1, Electrical simulation models — Wind turbines, *International Electrotechnical Commission*: Geneva, Switzerland, 2015.

[7] V. Gevorgian, Y. Zhang, and E. Ela, "Investigating the impacts of wind generation participation in interconnection frequency response," *IEEE Trans. Sustain. Energy*, Vol. 6, No. 3, pp. 1004-1012, Jul. 2015.

[8] F. Teng and G. Strbac, "Assessment of the role and value of frequency response support from wind plants," *IEEE Trans. Sustain. Energy*, Vol. 7, No. 2, pp. 586-595, Apr. 2016.

[9] L. Chang-Chien, W. Lin, and Y. Yin, "Enhancing frequency response control by DFIGs in the high wind penetrated power systems," *IEEE Trans. Power Syst.*, Vol. 26, No. 2, pp. 710-718, May 2011.

[10] L. Ruttledge, N. W. Miller, J. O'Sullivan, and D. Flynn, "Frequency response of power systems with variable speed wind turbines," *IEEE Trans. Sustain. Energy*, Vol. 3, No. 4, pp. 683-691, Oct. 2012.

[11] Z. Wu, W. Gao, J. Wang, and S. Gu, "A coordinated primary frequency regulation from permanent magnet synchronous wind turbine generation," in *IEEE Power Electronics and Machines in Wind Applications (PEMWA)*, pp. 1-6, Jul. 2012.

[12] H. Ye, W. Pei, and Z. Qi, "Analytical modeling of inertial and droop responses from a wind farm for short-term frequency regulation in power systems," *IEEE Trans. Power Syst.*, Vol. 31, No. 5, pp. 3414-3423, Sep. 2016.

[13] Y. Wang, G. Delille, H. Bayem, X. Guillaud, and B. Francois, "High wind power penetration in isolated power systems—assessment of wind inertial and primary frequency responses," *IEEE Trans. Power Syst.*, Vol. 28, No. 3, pp. 2412-2420, Aug. 2013.

[14] K. V. Vidyanandan and N. Senroy, "Primary frequency regulation by deloaded wind turbines using variable droop," *IEEE Trans. Power Syst.*, Vol. 28, No. 2, pp. 837-846, May 2013.

[15] R. You, J. Chai, X. Sun, J. Li, and W. Liu, "Experimental study of variable speed wind turbines based on electromagnetic couplers," *Proceedings of the CSEE*, Vol. 33, No. 3, pp. 92-98, Mar. 2013.

[16] R. You, B. Barahona, J. Chai, and N. A. Cutululis, "A novel wind turbine concept based on an electromagnetic coupler and the study of its fault ride-through capability," *Energies*, Vol. 6, No. 11, pp. 6120-6136, Nov. 2013.

[17] R. You, B. Barahona, J. Chai, and N. A. Cutululis, "Frequency support capability of variable speed wind turbine based on electromagnetic coupler," *Renewable Energy*, Vol. 74, pp. 681-688, Feb. 2015.

[18] J. Chen, Q. Zhou, J. Chai, D. Bi, X. Sun, and W. Liu, "VSCF wind turbine generator based on an electromagnetic coupler," *Journal of Tsinghua University (Science and Technology)*, Vol. 51, No. 3, pp. 361-366, Mar. 2011.

[19] R. You, B. Barahona, J. Chai, N. A. Cutululis, and X. Wu, "Improvement of grid frequency dynamic characteristic with novel wind turbine based on electromagnetic coupler," *Renewable Energy*, Vol. 113, pp. 813-821, Dec. 2017.

[20] R. You, J. Chai, X. Sun, and Y. Lin, "Variable speed wind turbine based on electromagnetic coupler and its experimental measurement," in *IEEE Power and Energy Society General Meeting / Conference & Exposition*, Jul. 2014.

[21] M. H. Hansen, A. Hansen, T. J. Larsen, S. Øye, P. Sørensen, and P. Fuglsang, "Control design for a pitch-regulated, variable speed wind turbine," *DTU Wind Energy*, Roskilde, Denmark, Tech. Rep. Risø-R-1500, Jan. 2005.

[22] J. Ekanayake and N. Jenkins, "Comparison of the response of doubly fed and fixed-speed induction generator wind turbines to changes in network frequency," *IEEE Trans. Energy Convers.*, Vol. 19, No. 4, pp. 800-802, Dec. 2004.

[23] L. Yang, H. Li, and X. Xiao, *LabVIEW program development and application*, Publishing House of Electronics Industry, pp. 261-264 (in Chinese), 2001.

Rui You was born in Qingdao, China, in 1984. He received his B.S. degree in Electrical Engineering from Qingdao University, Qingdao, China, in 2006; his M.S. degree in Electrical Engineering from Shanghai Jiao Tong University, Shanghai, China, in 2009; and his Ph.D. degree in Electrical Engineering from Tsinghua University, Beijing, China, in 2015. He joined Qingdao University in 2015, where he is presently working as an Associate Professor in the Department of Electrical Engineering. His current research interests include wind turbine control and wind power integration.

Jianyun Chai was born in Beijing, China, in 1961. He received his B.S. and Ph.D. degrees from the Department of Electrical Engineering, Tsinghua University, Beijing, China, in 1984 and 1989, respectively. Since 1989, he has been working at Tsinghua University, where he is presently a Professor in the fields of electric machinery and power electronics. His current research interests include wind energy generation, electric vehicle drives, integrated power and propulsion systems, and motion control.

Xudong Sun was born in Dalian, China, in 1965. He received his B.S. and Ph.D. degrees from the Department of Electrical Engineering, Harbin Institute of Technology, Harbin, China, in 1986 and 1992, respectively. Since 1992, he has been working at Tsinghua University, where he is presently an Associate Professor in the fields of electric machinery and power electronics. His current research interests include electric machines and their control, power electronics, electric drives, and renewable generation systems.

Daqiang Bi was born in Jilin Province, China, in 1973. He received his M.S. degree in Electrical Engineering from the Shenyang University of Technology, Shenyang, China, in 1999; and his Ph.D. degree from Tsinghua University, Beijing, China, in 2003, where he worked as a Post-Doctoral Researcher from August 2003 to June 2005. He is presently working as a Senior Engineer in State Key Laboratory of Power Systems and as the Director of the Laboratory on Power Electronics and Electric Machine Control, Department of Electrical Engineering, Tsinghua University. His current research interests include power system relay protection and the application of power electronics to power system.

Xinzhen Wu was born in Jiangsu Province, China, in 1964. He received his B.S. and Ph.D. degrees from Tsinghua University, Beijing, China, in 1986 and 2006, respectively; and his M.S. degree from Southeast University, Nanjing, China, in 1989, all in Electrical Engineering. He is presently working as a Professor in the Department of Electrical Engineering, Qingdao University, Qingdao, China. His current research interests include design, analysis and control of electric machines and their systems.